



1-(1-(4-hidroksibütül)-6-metil-4-fenil-2-tioksoheksahidropirimidin-5-il)etan-1-on bileşiğinin Moleküler Doking, ADME Analiz ve DFT Yöntemi ile Teorik Hesaplamalar

Efdal ÇİMEN^{1*}, Kenan GÖREN², Veysel TAHİROĞLU³, Ümit YILDIKO⁴

¹Kafkas University, Kars Vocational School, Chemistry and Chemical Processing Technologies, 36100, Kars

²Kafkas University, Faculty of Art and Sciences, Department of Chemistry, 36100, Kars

³Sirnak University, Health Sciences Faculty, Nursing Department, 7300, Şırnak

⁴Kafkas University, Department of Bioengineering, 36100, Kars

¹<https://orcid.org/0000-0003-2461-5870>

²<https://orcid.org/0000-0001-5068-1762>

³<https://orcid.org/0000-0003-3516-5561>

⁴<https://orcid.org/0000-0001-8627-9038>

*Sorumlu yazar: efdalcimen@gmail.com

Araştırma Makalesi

Makale Tarihiçesi:

Geliş tarihi: 06.10.2024

Kabul tarihi: 15.03.2025

Online Yayınlanma: 16.06.2025

Anahtar Kelimeler:

DFT

Moleküler doking

MEP

ADME

NBO

ÖZ

Gaussian 09W yazılımı kullanılarak, 1-(1-(4-hidroksibütül)-6-metil-4-fenil-2-tioksoheksahidropirimidin-5-il)etan-1-one (HMEP) bileşiğinin teorik olarak ideal moleküler yapısı incelenmiştir. Bileşiğin moleküler yapısı ve kimyasal reaktivitesi incelemek için, Yoğunluk Fonksiyonel Teorisi (DFT) kullanılarak hesaplandı. Kuantum kimyasal hesaplamalar, DFT(B3LYP/6-311G(d,p), DFT(B3LYP/LANL2DZ) metod ve temel setler kullanılarak yapıldı. HMEP molekülünün reaktif alanlarını belirlemek amacıyla moleküler elektrostatik potansiyel (MEP) haritaları oluşturuldu. Moleküler yük aktarımı için HOMO ve LUMO analizleri yapıldı. Molekülün stabilitesi, NBO analizi kullanılarak yük delokalizasyonu ve hiperkonjugatif etkileşimin bir fonksiyonu olarak incelenmiştir. Moleküler optimizasyon her iki yaklaşımda da aynı metod ve temel setlerle gerçekleştirildi. Çalışmanın devamında HMEP molekülünün moleküler analizi yapıldı. Emilim, dağılım ve metabolizma için uygun değerleri gösteren bileşiklerin ADME profilini tahmin etmek için SwissADME araçları kullanıldı. Bu araştırmanın sonuçları güvenli ve etkili bir farmakolojik ilaç üreten endüstride faydalı olabileceğini göstermektedir.

The Theoretical Calculations by DFT Method and Analysis ADME, Molecular Docking of 1-(1-(4-hydroxybutyl)-6-methyl-4-phenyl-2-thioxohexahydropyrimidin-5-yl)ethan-1-one (pyrimidine-thiones) Compound

Research Article

Article History:

Received: 06.10.2024

Accepted: 15.03.2025

Published online: 16.06.2025

Keywords:

DFT

Moleküler docking

MEP

ADME

NBO

ABSTRACT

Using Gaussian 09W software, the theoretically ideal molecular structure of 1-(1-(4-hydroxybutyl)-6-methyl-4-phenyl-2-thioxohexahydropyrimidin-5-yl)ethan-1-one (HMEP) compound was investigated. We investigated the compound's chemical reactivity and molecular structure using Density Functional Theory (DFT). Quantum chemical calculations were calculated using DFT(B3LYP/6-311G(d,p) and DFT(B3LYP/LANL2DZ) methods and basis sets. The reactive sites of the HMEP molecule were determined by creating molecular electrostatic potential (MEP) maps. In order to investigate molecular charge transfer, HOMO and LUMO analyses were done. By the use of NBO analysis, the stability of the molecule was examined in relation to charge hyperconjugative and delocalization interactions. In both cases, the same methodology and basis sets were used for molecular optimization. In continuation of the study, molecular analysis of the HMEP molecule was performed. SwissADME tools were used to predict the ADME profile of compounds showing appropriate values for absorption, distribution and

metabolism. The results of this research indicate that it can be useful in the industry producing safe and effective pharmaceutical drugs.

To Cite: Çimen E., Gören K., Tahiroğlu V., Yıldıkı Ü. The Theoretical Calculations by DFT Method and Analysis ADME, Molecular Docking of 1-(1-(4-hydroxybutyl)-6-methyl-4-phenyl-2-thioxohexahydropyrimidin-5-yl)ethan-1-one (pyrimidine-thiones) Compound. *Osmaniye Korkut Ata Üniversitesi Fen Bilimleri Enstitüsü Dergisi* 2025; 8(3): 1129-1145.

1. Introduction

The many biological characteristics of pyrimidine-containing substances are well-known. Alloxan, a pyrimidine derivative, was initially isolated by Brugnatelli in 1818, and it was later discovered that this chemical has antineoplastic qualities. Pyrimidine base nucleosides have been widely employed as antiviral and anticancer drugs. As of late, solid tumors and gastrointestinal cancer have been treated using combination therapies based on fluoropyrimidines and fluorouracil. It has been discovered that fluoropyrimidinones are metabolites of dihydropyrimidinones, which are α 1a-adrenergic receptor antagonists with subtype selectivity. One of the most well-known structures in nucleic acid chemistry is the pyrimidine entity (Dinakaran et al. 2012). According to clinical trials, the majority of medications used in cancer chemotherapy don't work well enough due to their ineffectiveness, selectivity, or different side effects. A class of chemotherapeutic drugs known as pyrimidine-based small molecules includes 5-FU, capecitabine, decitabine, gemcitabine, raltitrexed, floxuridine, tegafur, and more (Mustafa et al. 2018). These anticancer drugs block the right targets, causing apoptosis as they move through the cell cycle. In addition, system nitrogen, oxygen, and sulfur heteroatoms also contain tiny compounds based on pyrimidines. Organosulfur compounds are parts of tiny molecules based on pyrimidines. Thioanalogs of ketones are significant scaffolds in this context among the organosulfur derivatives (both natural and synthetic), from the perspectives of chemistry, medicine, and industry. The majority of organosulfur derivatives have been reported in the literature to be possible inhibitors of a number of important enzymes, demonstrating the significance of these class molecules in medicinal chemistry (Gularte et al. 2019; Yu and Jiang, 2023).

In this study, the Gaussian 09W program was used to perform initial calculations for 1-(1-(4-hidroksibutil)-6-metil-4-fenil-2-tioksoheksahidropirimidin-5-il)etan-1-one (HMEP) (Taslimi et al. 2018) molecule, which is a pyrimidine derivative. Firstly, the HMEP molecule was drawn using the ChemBioDraw program. Molecular optimization and electronic properties were calculated using (B3LYP/6-311G(d,p)), (B3LYP/LANL2DZ) methods and basis sets. The molecule used complies with drug similarity rules and exhibits acceptable ADME properties. A Molecular docking study was used to compare this molecule with the title compound, a new drug candidate, and to analyze the docking mechanism.

2. Materials and Methods

For initial calculations in the Gaussian 09W program, HMEP molecules were drawn in ChemBioDraw. Then, HMEP molecules were minimized using the Chem3D program. After the molecules were minimized, Gaussian 09W was used to calculate HMEP structure. The molecule was optimized through the use of gas phase (B3LYP/6-311G(d,p)), (B3LYP/LANL2DZ) method and basis sets. Using a

Schrödinger, LLC model on the Maestro Molecular Modeling platform, the ligand's mechanism and the precise binding site over the protein were determined through the molecular docking process. ADME analysis of HMEP molecule was performed using the SwissADME (<http://www.swissadme.ch>) online database. We used the Origin 2019 64-bit program to compare the Mulliken charges of the molecule graphically.

3. Results and Discussion

3.1. Structure Details and Analysis

Due to their accuracy and efficiency, DFT calculations are currently considered the most widely used computational techniques (Abdullah et al. 2024; Tahiroğlu et al. 2024). The Gaussian 09W program was used for all quantum chemistry calculations in this research. The HMEP molecule, the hybrid correlation functional (B3LYP) with the 6-311(d,p) and LANL2DZ basis sets, was utilized to optimize the compound's geometry. Electrons close to the nucleus are considered to be approximate effective nuclear potentials (ECPs) in very massive nuclei. This atom's behavior is significantly influenced by relativistic effects (Alghamdi et al. 2023; Kartal et al. 2024). We used the best known basis set, LANL2DZ, for our calculations. Table 1 lists the molecule's ideal bond length parameters as established by the B3LYP method, and 6-(311G(d,p)/LANL2DZ) basis sets. This optimization provides the least amount of energy to the molecule. Without taking energy into account, a method is presented to produce a good initial estimate of the transition path between specific initial and final states of a system. In aromatic phenyl rings, bond angles and bond lengths fall in the usual ranges.

The C-C bond lengths are 1.54-1.7 Å for 6-311G(d,p) and 1.37-1.54 Å for LANL2DZ, with values ranging from 1.26 to 1.46 Å for C-O. The aromatic ring has C-H lengths of 1.086–1.088 Å. All C-C-C angles are between 119° and 121°. When atoms are selected as dihedral bonds in the Gaussian 09W program, some dihedral angles give negative results in angle degrees. These calculated numbers were valued according to the atoms' positions and locations in the bonds. The differences between the values of LanL2DZ and 6-311G(d,p) are extremely small.

3.2. Mulliken Atomic Charges

Partial atomic charges are a useful indicator for understanding molecular properties and the mechanisms underlying chemical reactions, as they can show how shifting the molecular geometry affects the flow of electronic charges within the molecule (Gören et al. 2024). In order to learn more about the effects of electron delocalization and π -conjugation on the electronic charges over the atoms in the studied compound. Molecular docking analysis was performed to learn more about the effects of electron delocalization and π -conjugation on the electronic charges on the atoms in the studied molecule. B3LYP method and (6-311G(d,p)/LANL2DZ) basis sets were utilized to calculate the Mulliken atom. The calculated Mulliken values have been presented in Table 2.

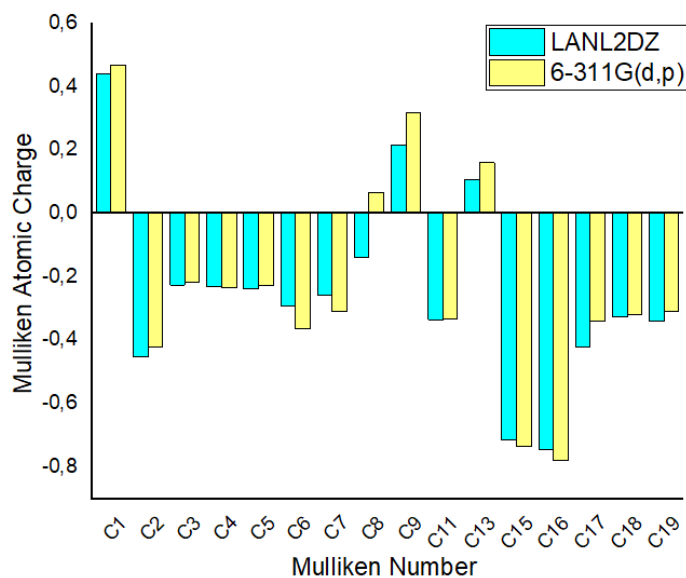
Table 1. The pyrimidine-thione molecule's bond lengths (Å) and bond angles (°) calculated theoretically

Bond Lengths	B3LYP/ 6-311G	B3LYP/ LANL2DZ	Bond Lengths	B3LYP/ 6-311G	B3LYP/ LANL2DZ
C20-O21	1.46529	1.46535	C11-N12	1.36165	1.36122
C1-C2	1.41207	1.41236	C11-N10	1.40337	1.40242
C2-C3	1.40748	1.40720	C8-C9	1.37428	1.37398
C3-C4	1.40814	1.40805	C11-S22	1.71682	1.73774
C4-C5	1.40870	1.40829	C8-C13	1.48978	1.48956
C6-C1	1.41263	1.41242	C13-O14	1.26386	1.26393
C1-C7	1.54123	1.54153	C9-N10	1.42562	1.42610
C7-N12	1.47225	1.47194	C9-C16	1.51789	1.51790
C5-C16	1.40682	1.40685	C5-H26	1.08770	1.08771
C7-C8	1.53242	1.53264	C18-H37	1.09899	1.09901
C17-N10	1.49036	1.49036	C13-C15	1.52801	1.52768
C17-C18	1.54318	1.54306	C18-C19	1.54343	1.54330
C13-O14	1.26386	1.26393	C19-C20	1.52941	1.52930
C2-H23	1.08684	1.08684	C4-H25	1.08750	1.08753
C5-H26	1.08770	1.08771	C3-H24	1.08751	1.08755
Bond Angles	B3LYP/ 6-311G	B3LYP/ LANL2DZ	BondAngles	B3LYP/ 6-311G	B3LYP/ LANL2DZ
C1-C2-C3	120.51791	120.50639	C11-N10-C9	121.45220	115.38839
C3-C4-C5	119.52932	119.51762	C15-C13-O14	117.48352	117.48645
C1-C7-N12	112.34350	112.38371	C8-C13-O14	118.50779	118.49798
N10-C11-N12	115.34350	115.61795	N10-C11-S22	124.14110	124.23937
Planar Bond Angles	B3LYP/ LANL2DZ	Planar Bond Angles	B3LYP/ 6-311G	B3LYP/ LANL2DZ	
C1-C2-C3-C4	-0.35882	-0.39674	C7-N12-C11-N10	-18.64753	-18.84226
C1-C7-C8-C9	103.68595	103.05891	C7-C8-C13-O14	-20.08705	-19.852272
C1-C7-N12-C11	-92.93011	-92.20051	C7-C8-C13-C15	154.54595	154.85508
C7-C8-C9-N10	-0.14948	-0.10764	C9-C8-C13-O14	158.36122	158.52735
C17-C18-C19-C20	-177.68734	-177.76847	C18-C19-C20-O21	-177.31779	-177.25439
C9-N10-C11-S22	170.095315	169.53244	C7-N12-C11-S22	162.69431	162.53115

The Mulliken atomic charge distribution shows that the oxygen atom attached to the aromatic ring has negative O14 (-0.233) and O21 (-0.472) charges for B3LYP/6-311G(d,p) and O14 (-0.233) and O21 (-0.485) charges for B3LYP/LANL2DZ, respectively. The positive charge is present in the H atom that is joined to the aromatic ring. It was observed that some atoms were negative, and some were positive. The Mulliken charges of some C atoms of the HMEP molecule calculated using the methods of the study were compared in graphical form in Figure 1. When we examined Figure 1, we observed that the Mulliken charges took similar values.

Table 2. Mulliken atomic charges of HMEP molecule

ATOMS	B3LYP/ 6-311G(d,p)	B3LYP/ LANL2DZ	ATOMS	B3LYP/ 6-311G(d,p)	B3LYP/ LANL2DZ
C1	0.441	0.469	H23	0.226	0.266
C2	-0.452	-0.422	H24	0.218	0.220
C3	-0.226	-0.218	H25	0.220	0.222
C4	-0.230	-0.234	H26	0.217	0.218
C5	-0.239	-0.227	H27	0.226	0.235
C6	-0.291	-0.364	H28	0.281	0.330
C7	-0.258	-0.309	H29	0.252	0.223
C8	-0.139	0.067	H30	0.238	0.249
C9	0.217	0.318	H31	0.186	0.225
C11	-0.335	-0.332	H32	0.239	0.237
C13	0.108	0.160	H33	0.229	0.262
C15	-0.714	-0.736	H34	0.247	0.231
C16	-0.745	-0.781	H35	0.224	0.206
C17	-0.421	-0.339	H36	0.230	0.256
C18	-0.327	-0.318	H37	0.113	0.200
C19	-0.339	-0.310	H38	0.236	0.176
C20	-0.323	-0.293	H39	0.193	0.191
N10	-0.088	-0.138	H40	0.193	0.209
N12	-0.233	-0.309	H41	0.185	0.182
O14	-0.233	-0.288	H42	0.184	0.174
O21	-0.472	-0.485	H43	0.343	0.347
S22	-0.172	-0.048	H44	0.194	0.273

**Figure 1.** The HMEP molecule's Mulliken Atomic Charges

3.3. HOMO and LUMO Analysis

The DFT method offers useful insights into the molecule's structural characteristics. The location and energy of the molecule's HOMO-LUMO orbitals play a major role in reactivity, and electron exchange results in the involvement of active sites in reactions (Gören et al. 2024; Tahiroğlu and Çimen, 2024). Quantum chemical structures, including the ionization potential (IP) and energy gap (ΔE), were calculated using the energies of the highest occupied (E_{HOMO}) and lowest unoccupied (E_{LUMO}) molecular

orbitals. By estimating the band gap, the lowest unoccupied molecular orbital (LUMO), and the highest occupied molecular orbital (HOMO), one can determine the basic electronic parameters of the molecule (Tahiroğlu et al. 2024). The frontier orbitals are LUMO, which has enough space to take electrons and function as an electron acceptor, and HOMO, which can act as an electron donor. The densities of the HOMO and LUMO orbital representations for the HMEP molecule are displayed in Figures 2, 3. As illustrates in Table 3, HOMO -5.7676 eV, LUMO -2.0294 eV were calculated to the 6-311G(d,p) basis set and HOMO -5.7742 eV, LUMO -2.0653 eV were calculated for the LANL2DZ basis sets. For the other orbitals; For B3LYP-6-311G(d,p) method, HOMO-1 -5.9276 eV, LUMO+1 -0.6084 eV and for B3LYP/LANL2DZ method, HOMO-1 -5.7742 eV, LUMO+1 -0.6395 eV were calculated. Because characteristics like energy and molecular orbitals (HOMO-LUMO) are crucial for quantum chemistry and highly helpful to physicists and chemists. Frontier molecular orbital analysis defines an electron hit from HOMO to LUMO. Electron affinity and ionization potential are directly related to HOMO and LUMO energies, respectively. The potential charge transfer during interaction with molecules is described by the LUMO and HOMO energy gaps (Yildiko et al. 2021; Gören et al. 2024a). Molecules with soft expression, high chemical reactivity and low kinetic stability are associated with frontier orbital fields. The interactions of the molecule with other compounds are determined by the HOMO and LUMO orbitals. It also helps in characterizing the kinetic stability, chemical reactivity and band gap (Suvitha et al. 2015). A molecule with an orbital space has polarization, hardness, electronegativity and other reactivity indices indicated by a small boundary.

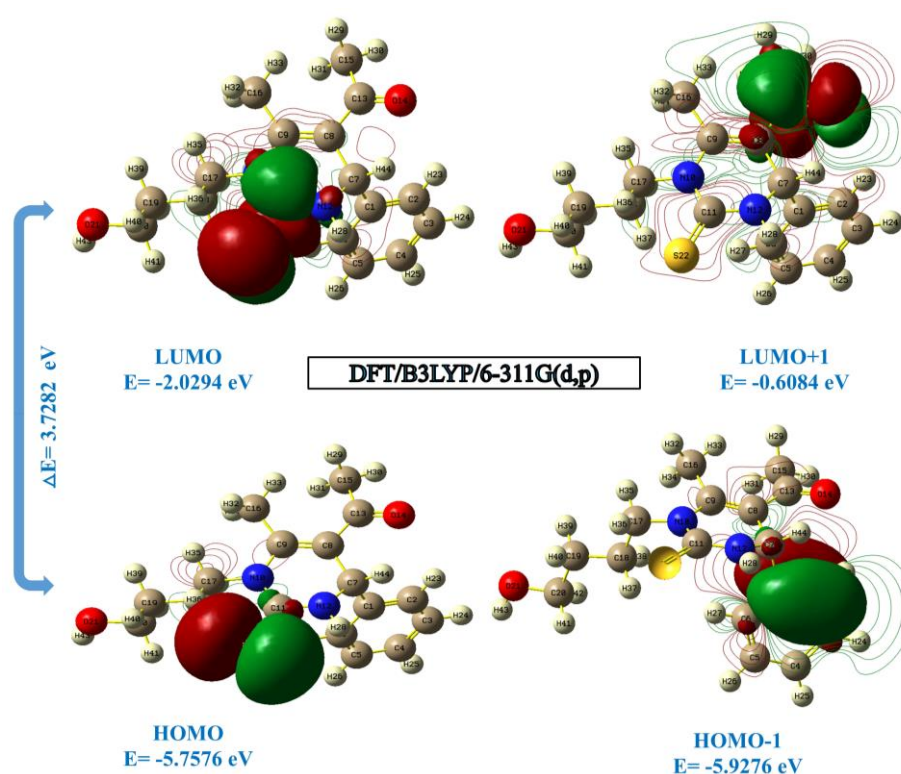


Figure 2. The boundaries molecular orbitals B3LYP/6-311G(d,p) method and basis set of the HMEP molecule

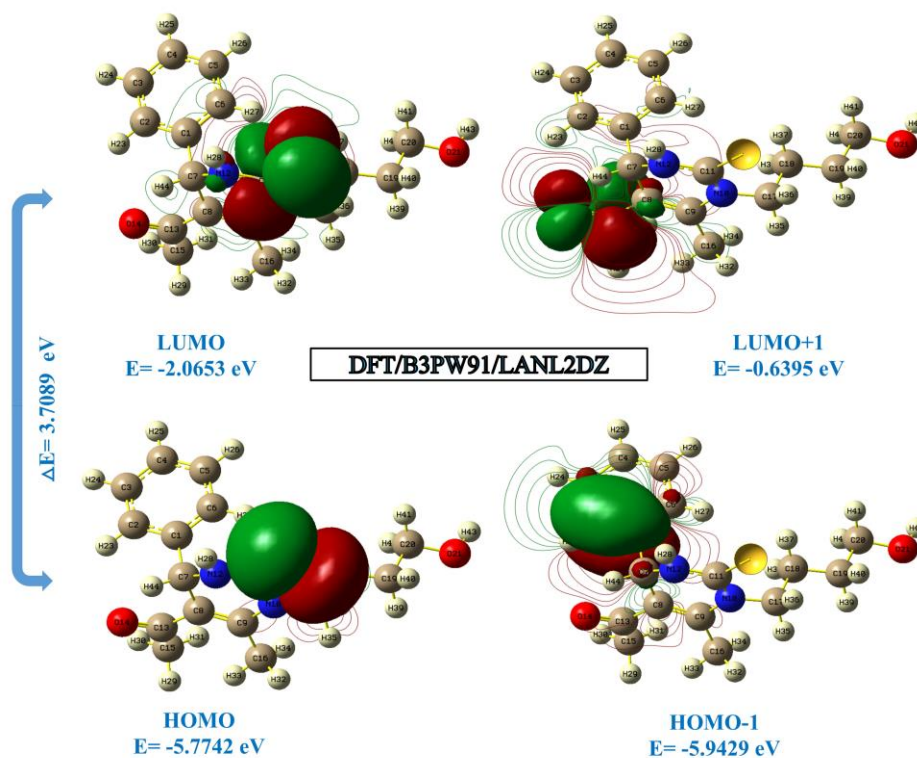


Figure 3. The boundaries molecular orbitals B3LYP/LANL2DZ method and basis set of the HMEP molecule

Table 3. Quantum chemical parameters (in eV) of the HMEP molecule calculated using the (B3LYP/6-311G(d,p)), (B3LYP/LANL2DZ) methods and basis sets

Molecules Energy		DFT/ B3LYP/ 6-311G(d,p)	DFT/B3LYP/ LANL2DZ
E_{LUMO}		-2.0294	-2.0653
E_{HOMO}		-5.7576	-5.7742
$E_{\text{LUMO}+1}$		-0.6084	-0.6395
$E_{\text{HOMO}-1}$		-5.9276	-5.9429
Energy Gap	$(\Delta E) E_{\text{HOMO}}-E_{\text{LUMO}} $	3.7282	3.7089
Ionization Potential	$(I=-E_{\text{HOMO}})$	5.7576	5.7742
Electron Affinity	$(A=-E_{\text{LUMO}})$	2.0294	2.0653
Chemical hardness	$(\eta=(I-A)/2)$	1.8641	1.8545
Chemical softness	$(s=1/2\eta)$	0.9321	0.9272
Chemical Potential	$(\mu=-(I+A)/2)$	-3.8935	-3.9198
Electronegativity	$(\chi=(1+A)/2)$	1.5147	1.5327
Electrophilicity index	$(\omega=\mu^2/2\eta)$	4.0661	4.1426

3.4. Molecular Electrostatic Potential (MEP)

It is a useful technique to look at molecular charge distributions and variable charge regions (Gören et al. 2024b). The MEP surface was drawn to the HMEP compound in Figure 4. MEP mapping of molecular electrostatic potential is a very important tool for studying various aspects of molecular structure (Gören and Yıldiko 2024). To comprehend hydrogen bonding interactions as well as electrophilic and nucleophilic reactions on organic molecules, MEP is frequently used as a reactivity map (Yıldiko et al. 2021). Electrophilic attacks can target molecules with negative electrostatic potential. The electrostatic potential at the surface is represented by a range of colors from blue to red.

The MEP map of the HMEP molecule shows the red areas where the nitrogen atoms are negatively positioned. The relatively large region around the nitrogen atoms of the HMEP molecule is a dark red, highly negative potential region that allows electrophilic interaction. The strongest positive charge is found on the hydrogen atom (dark blue). The nearly neutral potential in the aromatic ring is given primarily with green tones.

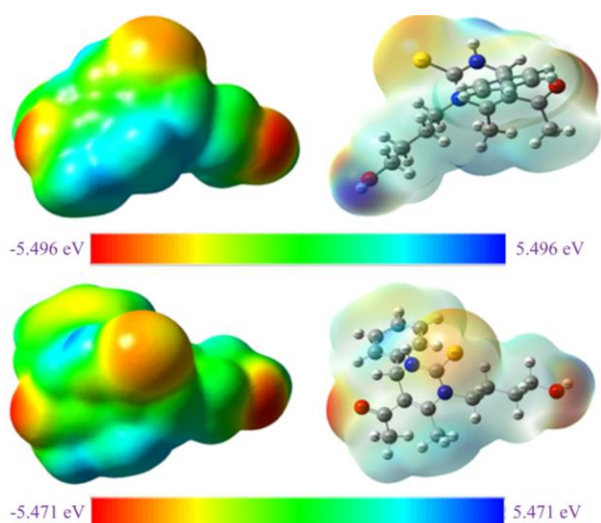


Figure 4. Molecular electrostatic potential surface of HMEP using (B3LYP/6-311G(d,p)), (B3LYP/LANL2DZ) methods and basis sets

3.5. Non-Linear Optical Properties (NLO)

The macroscopic non-local optical activity (NLO) of organic materials is determined by the density of individual organic chromophores, their non-centrosymmetric alignment, and their hyperpolarizability (Tahiroğlu et al. 2024). The nonlinear optical properties of the molecule were calculated using the (B3LYP/6-311G(d,p)), (B3LYP/LANL2DZ) methods and basis sets. The results have been shown in Table 4 in both atomic and electrostatic units. These characteristics included the average polarization α , polarization anisotropy α_{ij} , first-order hyperpolarization anisotropy β_{ijk} , dipole moment μ_i component, and total static dipole moment μ . With the 6-311G(d,p) basis set, $\mu=5.2054$ D, $\alpha=-155.6472$ a.u and $\beta=2.76 \times 10^{-30}$ esu and with the LANL2DZ basis set, $\mu=3.6526$ D, $\alpha=-148.2117$ a.u. and $\beta=2.69 \times 10^{-30}$ esu were calculated. The estimated values of $\alpha=-175.055$ and -169.8000 a.u in the HMEP molecule can serve as evidence that the material is NLO.

$$\mu (\mu_x^2 + \mu_y^2 + \mu_z^2)^{1/2} \quad (1)$$

$$\beta_{Total} = (\beta^2_x + \beta^2_y + \beta^2_z)^{1/2} \quad (2)$$

$$= [(\beta_{xxx} + \beta_{xyy} + \beta_{xzz})^2 + (\beta_{yyy} + \beta_{yxx} + \beta_{yzz})^2 + (\beta_{zzz} + \beta_{zxx} + \beta_{zyy})^2]^{1/2} \quad (3)$$

Table 4. The HMEP molecule's polarizability (au), components, dipole moments (Debye), and total value calculated with (B3LYP/6-311G(d,p)), (B3LYP/LANL2DZ) methods and basis sets

Parameters	B3LYP/ 6-311G(d,p)	B3LYP/ LANL2DZ	Parameters	B3LYP/ 6-311G(d,p)	B3LYP/ LANL2DZ
μ_x	0.4891	-2.0382	β_{xxx}	-10.3898	-64.1882
μ_y	-0.0111	2.8296	β_{yyy}	-2.2931	67.2454
μ_z	-5.1823	-1.0857	β_{zzz}	-66.0113	-7.1371
$\mu(D)$	5.2054	3.6526	β_{xyy}	44.1846	-38.1341
α_{xx}	-155.6472	-148.2117	β_{xxy}	91.4034	-118.6383
α_{yy}	-125.0630	-135.5206	β_{xxz}	-28.3008	-86.3614
α_{zz}	145.7591	-133.6442	β_{xzz}	-11.0703	21.3886
α_{xy}	0.1861	0.5273	β_{yzz}	-2.4869	-6.9705
α_{xz}	-9.2531	8.8203	β_{yyz}	-46.5252	16.7187
α_{yz}	-2.6903	-1.7928	β_{xyz}	-23.1435	-15.1085
α (au)	175.055	-169.8000	β (esu)	2.76×10^{-30}	2.69×10^{-30}

3.6. NBO Analysis

Natural bond orbital (NBO) analysis is used to study charge transfer interactions within bonds (Bağlan et al. 2023b). NBO of HMEP compound was analyzed using B3LYP/6-311G(d,p) method and basis set. The components of the off-diagonal NBO Fock matrix $F(ij)$ are computed utilizing the interaction energy. You can use the second-order perturbation method to calculate it (Yildiko and Tanriverdi, 2021). NBO analysis reveals that a single Lewis formula-corresponding stable molecular species can be fully represented by a chemical bond by using monocentric lone pairs and eccentric bonds. Valence antibonds (BD) can be observed as non-Lewis structures, non-empty valence bonds (LP) and extra valence shell Rydberg (RY*) orbitals. The occupancy of these Lewis-type NBOs (lone pairs and bonds) can be used to determine the absence of Lewis-type NBOs expressing the density matrix. The analyzed results have been given in Table 5. Intramolecular interactions are observed as an increase in the electron density (ED) in the antibond orbitals, which weakens the corresponding bonds (C-O). The occupancy of σ bonds is higher than that of σ^* bonds, allowing for greater localization. The intramolecular hyperconjugative interaction of the distribution of $\pi(C2-C3)$ electrons in the ring, Table 5 shows how the intermolecular hyperconjugative interaction is propagated by (C5-C6) to $\sigma^*(C6-C8)$, leading to a stabilization of 12.39 KJ/mol. The electron donation from $\pi^*(C13-O14)$ to the antibonding acceptor from $\pi(C8-C9)$ is the highest and most significant energy of the molecule having a stabilization energy of 18.02 KJ/mol. These values increased conjugation leading to strong localization.

Table 5. The HMEP molecule's selected NBO results calculated using the basis set and 6-311G(d,p) basis set

NBO(i)	Type	Occupancies	NBO(j)	Type	Occupancies	E(2) ^a (Kcal/mol)	E (j)-E(i) ^b (a.u.)	F (i, j) ^c (a.u)
C1-C2	π	1.81487	C3-C4	π^*	1.82516	11.43	0.31	0.053
C1-C6	σ	1.96937	C2-H23	σ^*	1.97771	4.17	1.13	0.061
C1-C7	σ	1.96436	C2-C3	σ^*	1.97308	3.55	1.01	0.054
C2-C3	σ	1.97308	C1-C7	σ^*	1.96426	7.19	0.97	0.075
C2-H23	σ	1.97771	C1-C6	σ^*	1.96937	7.69	0.92	0.077
C3-C4	π	1.82516	C1-C2	π^*	1.81487	11.43	0.31	0.054
C3-H24	σ	1.97779	C4-C5	σ^*	1.97765	6.50	0.92	0.069
C4-C5	σ	1.97765	C3-H24	σ^*	1.97779	4.20	1.14	0.062
C4-H25	σ	1.97781	C2-C3	σ^*	1.97308	6.72	0.91	0.070
C5-C6	π	1.80692	C1-C2	π^*	1.81487	12.39	0.31	0.055
C5-H26	σ	1.97794	C1-C6	σ^*	1.96937	6.90	0.91	0.071
C6-H27	σ	1.97742	C4-C5	σ^*	1.97765	6.32	0.91	0.068
C7-C8	σ	1.96697	C9-C16	σ^*	1.97352	5.54	0.95	0.065
C7-N12	σ	1.97668	C11-S22	σ^*	1.97370	3.80	0.84	0.053
C7-H44	σ	1.90298	C8-C9	σ^*	1.97466	13.25	0.49	0.073
C8-C9	π	1.85950	C13-O14	π^*	1.96864	18.02	0.29	0.065
C8-C13	σ	1.96762	C9-N10	σ^*	1.97012	7.31	0.92	0.074
C9-N10	σ	1.97012	C8-C13	σ^*	1.96762	4.05	1.11	0.060
C9-C16	σ	1.97352	C7-C8	σ^*	1.96697	6.76	1.00	0.074
N10-C11	σ	1.97767	C9-C16	σ^*	1.97352	3.50	1.08	0.055
N10-C17	σ	1.97081	C11-N12	σ^*	1.98008	4.41	1.01	0.060
C11-N12	σ	1.98008	C1-C7	σ^*	1.96426	4.13	1.14	0.062
C11-S22	π	1.96776	C11-S22	σ^*	1.97370	5.23	1.04	0.067
N12-H28	σ	1.96467	C11-S22	σ^*	1.93370	1.92	1.26	0.044
C13-O14	π	1.96864	C8-C9	π^*	1.85950	6.17	0.39	0.046
C15-H29	σ	1.69799	C8-C13	σ^*	1.96762	4.31	0.87	0.055
C17-H36	σ	1.98281	C18-H38	σ^*	1.97593	3.17	1.07	0.052
C20-H42	σ	1.98782	C19-H40	σ^*	1.97899	3.12	1.04	0.051

3.7. Molecular Docking Studies

Molecular docking technique is in silico method utilized to identify the mutual effect between proteins and ligands (Bağlan et al. 2023a; Yildiko and Tanriverdi 2022). The protein crystal structures of the enzymes required for the docking analysis of the HMEP compound (PDB:3OG7 and PDB:3WIG) were taken from the Protein Data Bank (<http://www.rcsb.org>). In the docking analysis, the docking scores of the HMEP compound were calculated as -7.10 cal/mol for PDB:3OG7 and -6.90 cal/mol for PDB:3WIG and these values have been shown in Table 6. the HMEP molecule and the ligands' interactions' visualized findings of and 2D, 3D images have been given in Figures 5 and 6.

Table 6. HMEP molecule's docking score PDB: 3OG7 and PDB: 3WIG

Compound	Docking Score	
	(PDB: 3OG7)	(PDB: 3WIG)
HMEP	-7.40	-6.90

For 3OG7 enzyme is hydrogen bonded to benzene alkyl ASP:209 (6.84 Å), and ASP-209 (5.12 Å) by conventional hydrogen bonds. Pi-alkyl VAL-83 (5.71 Å) is bound to LEU-75 (5.90 Å), LEU-198 (5.04

Å), ALA-96 (6.83 Å), negative donor-donor is bound to HIS-146 (3.18 Å), MET-147 (4.59). GLY-78, GLY-150, VAL-82, SER-195, GLY-76, LEU-198, and LEU-75 are Van Der Waals bonds.

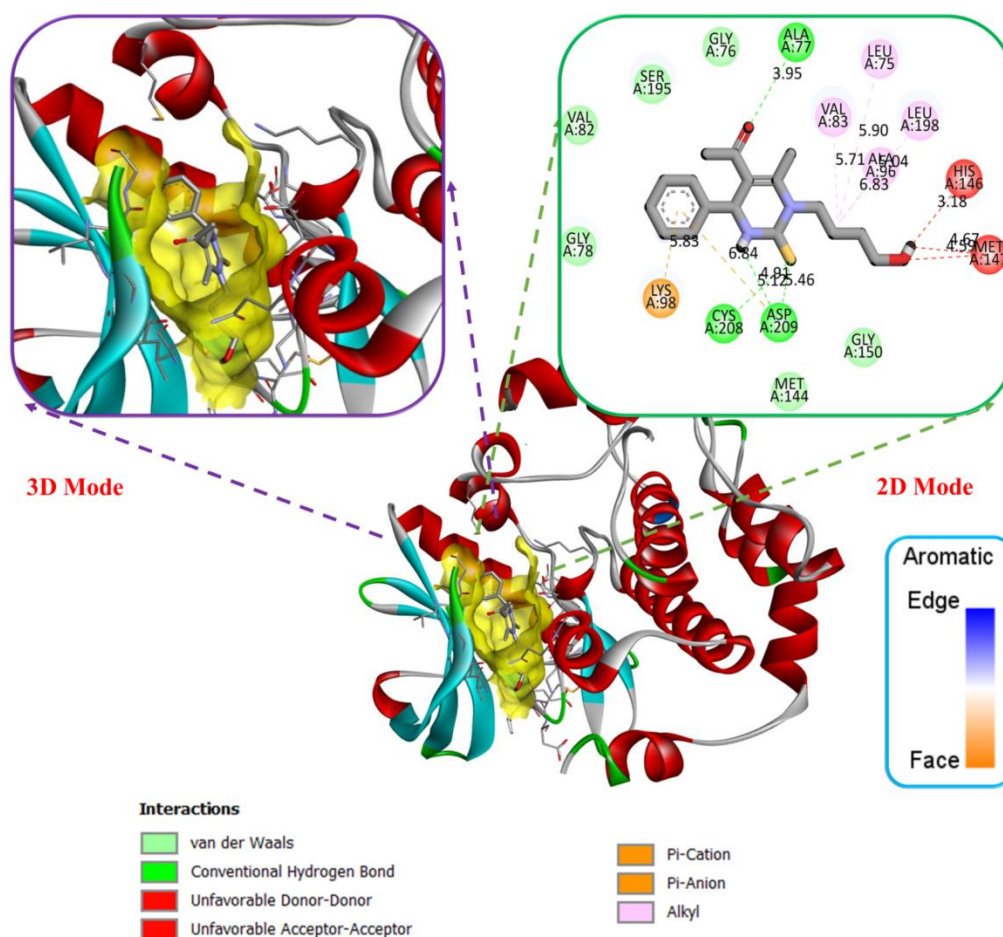


Figure 5. The interaction's 3D and 2D representation between 3OG7 enzyme and HMEP compound

For 3WIG enzyme is hydrogen bonded to the HMEP molecule of SER-213 (3.86 Å), VAL-212 (4.18 Å), and PHE-210 (3.20 Å), conventional hydrogen bonds for 3OG7. Pi-alkyl bonds to ILE-142 (5.35 Å), LYS-98 (5.50 Å), and benzene alkyl ARG-190 (6.42 Å). ASN-222, MET-220, ASN-196, LEU-119, LEU-116, LEU-216, and GLY-211 are van der Waals bonds.

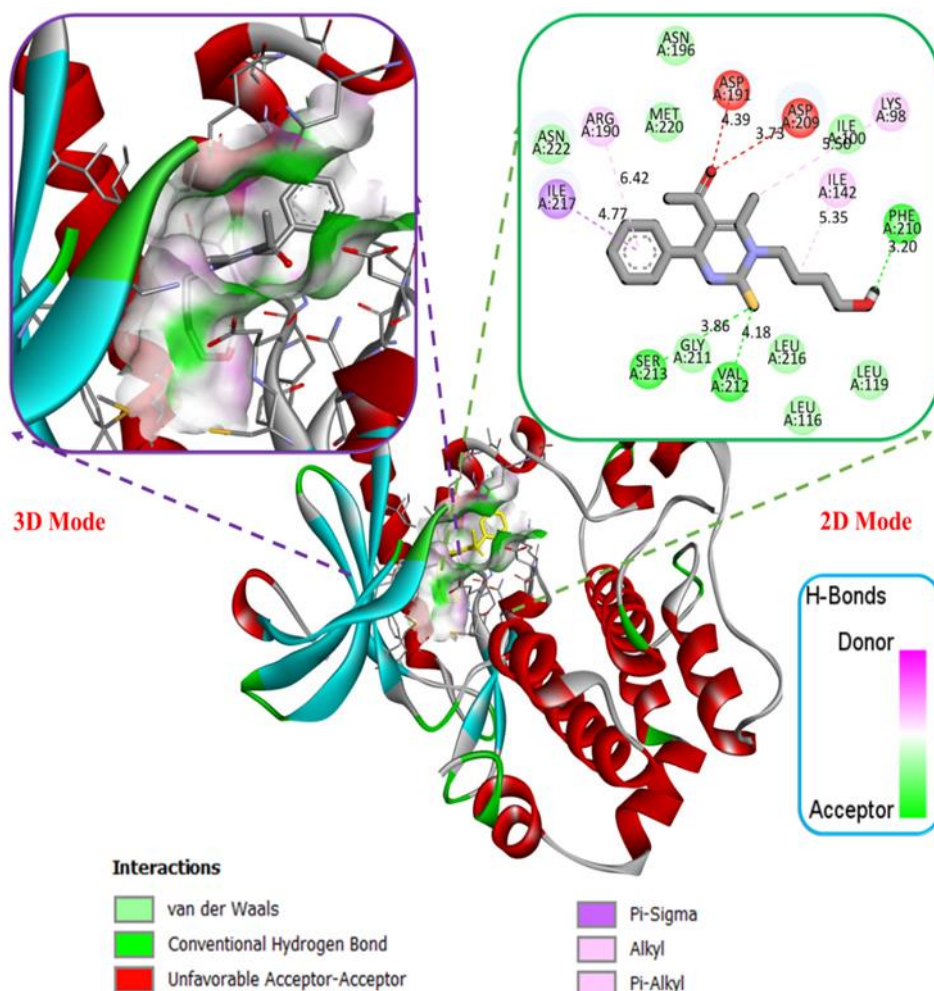


Figure 6. The interaction's 3D and 2D representation between 3WIG enzyme and HMEP compound

3.8. ADME Analysis

The extent of the ADME process is significantly influenced by the structural and physicochemical properties of the drug, including its shape, lipophilicity, solubility, dissociation constant, protein binding, hydrogen bonding, and molar fractionation (Bağlan et al. 2023). Lipophilicity is an important factor that defines the efficacy of a drug candidate and can have a major impact on its pharmacokinetic properties. Numerous studies have clarified the relationship between lipophilicity and pharmacokinetic properties (Kassel, 2004; Bağlan et al. 2022). Due to the lipid-based nature of biological targets, there is an increasing need to develop highly lipophilic drugs to achieve the required levels of drug efficacy and selectivity (Khodja et al. 2020). Drug development must take oral bioavailability into account (Bağlan et al. 2022). Lipinski's Rule of Five provides information on oral bioavailability and drug similarity by evaluating molecular weight, partition coefficient (logP), hydrogen bond acceptors, and donors (Chen et al. 2020). Veber extended this rule by adding variables for drug bioavailability such as topological polar surface area (TPSA) and number of rotatable bonds (nRB). The biological and chemoinformatic properties of this ligand molecule were investigated using the web-based server SwissADME (<http://www.swissadme.ch/index.php>). There are some criteria such as Lipinski's five criteria, Veber and Egan criteria to determine whether the compounds have a drug-like structure and

their activity in living organisms (Chagas et al. 2018). In this study, the compound's drug-like characteristics mentioned in the title were looked into utilizing Lipinski criteria. Lipinski's rule of five is an analysis method to calculate the drug-likeness of the compound and also to determine whether a chemical compound with a certain pharmacological or biological activity can be used as an active and orally active drug in humans (Nogara et al. 2015). Table 7 shows that it complies with the Lipinski requirements of MW 318.43 g/mol (<500), lipophilicity coefficient LogP 2.72 (≤ 5), H-acceptor 2 (≤ 5), H-donor 2 (<10) and Topological PSA 84.66 (<140). Figure 7 shows the physicochemical properties and color regions of the HMEP molecule. In the TPSA maps, polar regions are shown in red and non-polar regions are shown in gray. As a result, it is clear that the red colored patches become smaller and smaller as (1) and (2) change. The graphical representation of the HMEP molecule in the form of a boiled egg graph is visually depicted in Figure 8. Blood-Brain Barrier Penetration (BBB: 0956): Category 1: BBB+; Category 0: BBB-; The output value is the probability of being BBB+. Human Intestinal Absorption (0.341) Category 1: HIA+ (HIA<30%); Category 0: HIA- (HIA<30%); The output value is the probability of being HIA+. Pgp-substrate (0.005): The output value is the probability of being Pgp-substrate.

Table 7. Physicochemical and lipophilicity of HMEP molecule

Code	Lipophilicity consensus log P	Physico-chemical properties								
		MW ^a g/mol	Heavy Atoms	Aromatic heavy atoms	Rot. bond	H-acceptor bond	H-donor bond	MR ^b	TPSA ^c (Å ²)	% ABS ^d
HMEP	2.72	318.43	22	6	6	2	2	99.57	84.66	79.79

^aMW, molecular weight; ^cTPSA, topological polar surface area; ^bMR, molar refractivity; ^dABS%: absorption percent $ABS\% = 109 - [0.345 \times TPSA]$.

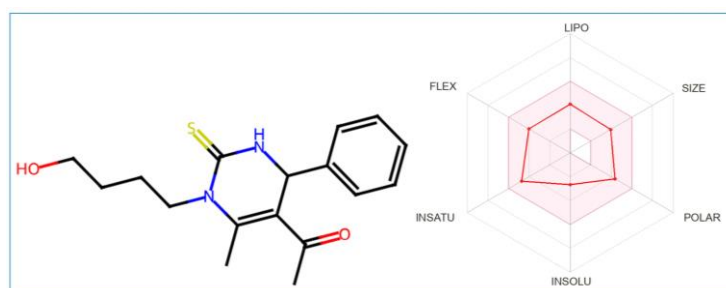


Figure 7. Color regions and physicochemical parameters of the HMEP molecule

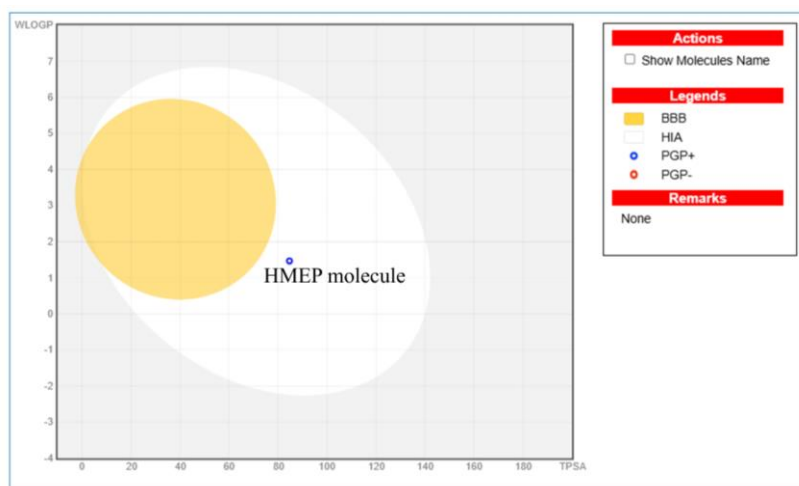


Figure 8. Boiled graph representations of HMEP molecule

4. Conclusion

In this study, theoretical calculations of the HMEP molecule were performed using LANL2DZ and 6-31G(d,p) basis sets. Bond lengths, bond angles and dihedral angles were calculated with this method and basis sets. In addition, NLO, MEP, HOMO-LUMO and Mulliken charges were calculated with this method and basis sets. Based on the same method and theoretical calculations, polarity ($\alpha = -175.055$ au and $\alpha = 169.800$ au) and static higher order polarity ($\beta = 2.76 \times 10^{-30}$ esu and $\beta = 2.69 \times 10^{-30}$ esu) values were calculated. In addition, ADME analysis was performed in our study and significant changes were observed in TPSA and logPow values. According to Lipinski's rules, it gave positive results for ADME analysis. Lastly, molecular docking analysis was used in our study to investigate the binding location and ligand activity on the proteins (PDB-CODE: 3OG7) and (PDB-CODE: 3WIG) that cause melanoma cancer. After determining the most suitable position for total ligand-enzyme docking, binding approaches were investigated for a deeper comprehension of the inhibitory procedures. According to the study, the shift scores for binding affinity with 3OG7 and 3WIG were calculated as -6.90 and -7.40 kcal/mol, respectively. The binding receptor score of 3OG7 was more effective than 3WIG enzyme with -7.40 kcal/mol. Considering the therapeutic potential of this molecular structure, we think that new drugs targeting melanoma cancer can be created.

Compliance with ethical standards

The authors declare that they have no conflict of interest.

Summary of researchers' contribution declaration

The authors affirm that their contributions to the essay were equal.

References

Abdullah A., Tanriverdi AA., Khan AA., Lee SJ., Park JB., Kim YS., Yildiko U., Min K., Alam M.
Selenium-substituted conjugated small molecule: Synthesis, spectroscopic, computational

- studies, antioxidant activity, and molecular docking. *Journal of Molecular Structure* 2024; 1304: 137694.
- Alghamdi S., Abbas F., Hussein R., Alhamzani A., El-Shamy N. Spectroscopic characterization (IR, UV-Vis), and HOMO-LUMO, MEP, NLO, NBO analysis and the antifungal activity for 4-bromo-N-(2-nitrophenyl) benzamide; using DFT modeling and In silico molecular docking. *Journal of Molecular Structure* 2023; 1271: 134001.
- Bağlan M., Gören K., Çakmak İ. Theoretical investigation of ¹H and ¹³C NMR Spectra of diethanol Amine dithiocarbamate RAFT agent. *Journal of the Institute of Science and Technology* 2022; 12(3): 1677-1689.
- Bağlan M., Gören K., Yıldıkı Ü. DFT computations and molecular docking studies of 3-(6-(3-aminophenyl)thiazolo[1,2,4]triazol-2-yl)-2H-chromen-2-one(ATTC) molecule. *Hittite Journal of Science and Engineering* 2023a; 10(1): 11-19.
- Bağlan M., Gören K., Yıldıkı Ü. HOMO–LUMO, NBO, NLO, MEP analysis and molecular docking using DFT calculations in DFPA molecule. *International Journal of Chemistry and Technology* 2023b; 7(1): 38-47.
- Bağlan M., Yıldıkı Ü., Gören K. Computational investigation of 5,5',7'-trihydroxy-3,7-dimethoxy-4'-4''-O-biflavone from flavonoids using DFT calculations and molecular docking. *Adıyaman University Journal of Science* 2022; 12(2): 283-298.
- Bağlan M., Yıldıkı Ü., Gören K. DFT calculations and molecular docking study in 6-(2''-pyrrolidinone-5''-Yl)-(-) epicatechin molecule from flavonoids. *Eskişehir Teknik Üniversitesi Bilim ve Teknoloji Dergisi B - Teorik Bilimler* 2023; 11(1): 43-55.
- Chagas CM., Moss S., Alisaraie L. Drug metabolites and their effects on the development of adverse reactions: revisiting lipinski's rule of five. *International Journal of Pharmaceutics* 2018; 549(1): 133-149.
- Chen X., Li H., Tian L., Li Q., Luo J., Zhang Y. Analysis of the physicochemical properties of acaricides based on lipinski's rule of five. *Journal of Computational Biology* 2020; 27(9): 1397-1406.
- Dinakaran VS., Jacob D., Mathew JE. Synthesis and biological evaluation of novel pyrimidine-2(1H)-ones/thiones as potent anti-inflammatory and anticancer agents. *Medicinal Chemistry Research* 2012; 21(11): 3598-3606.
- Gören K., Bağlan M., Tahiroğlu V., Yıldıkı Ü. Theoretical calculations and molecular docking analysis of 4-(2-(4-bromophenyl)hydrazineylidene)-3,5-diphenyl-4H-pyrazole molecule. *Journal of Advanced Research in Natural and Applied Sciences* 2024; 10(4): 786-802.
- Gören K., Bağlan M., Yıldıkı Ü. Antimicrobial, and antitubercular evaluation with adme and molecular docking studies and dft calculations of (z)-3-((1-(5-amino-1,3,4-thiadiazol-2-yl)-2-phenylethyl)imino)-5-nitroindolin-2-one schiff base. *Karadeniz Fen Bilimleri Dergisi* 2024a; 14(4): 1694-1708.

- Gören K., Bağlan M., Yıldiko Ü. Melanoma cancer evaluation with adme and molecular docking analysis, Dft calculations of (e)-methyl 3-(1-(4-methoxybenzyl)-2,3-dioxindolin-5-yl)-acrylate molecule. *Journal of the Institute of Science and Technology* 2024b; 14(3): 1186-1199.
- Gören K., Yıldiko Ü. Aldose reductase evaluation against diabetic complications using ADME and molecular docking studies and DFT calculations of spiroindoline derivative molecule. *Süleyman Demirel Üniversitesi Fen Bilimleri Enstitüsü Dergisi* 2024; 28(2): 281-292.
- Gularte MS., Anghinoni JM., Abenante L., Voss GT., de Oliveira RL., Vaucher RA., Luchese C., Wilhelm EA., Lenardão EJ., Fajardo AR. Synthesis of chitosan derivatives with organoselenium and organosulfur compounds: characterization, antimicrobial properties and application as biomaterials. *Carbohydrate Polymers* 2019; 219: 240-250.
- Kartal B., Tanriverdi AA., Yıldiko U., Tekes AT., Çakmak I. Polyimide synthesis and characterizations: DFT-assisted computational studies on structural units. *Iranian Polymer Journal* 2024: 1-23.
- Kassel DB. Applications of high-throughput ADME in drug discovery. *Current Opinion in Chemical Biology* 2004; 8(3): 339-345.
- Khodja IA., Boulebd H., Bensouici C., Belfaitah A. Design, synthesis, biological evaluation, molecular docking, DFT calculations and in silico ADME analysis of (benz) imidazole-hydrazone derivatives as promising antioxidant, antifungal, and anti-acetylcholinesterase agents. *Journal of Molecular Structure* 2020; 1218: 128527.
- Mustafa M., Zreid MS., Abadlehb MM. One-pot synthesis of model 1H, 1'H-5, 5'-Bi (1, 2, 4-triazoles). *Heterocycles* 2018; 96(6): 1080-1087.
- Nogara PA., Saraiva RdA., Caeran Bueno D., Lissner LJ., Lenz Dalla Corte C., Braga MM., Rosemberg DB., Rocha JBT. Virtual screening of acetylcholinesterase inhibitors using the lipinski's rule of five and zinc databank. *BioMed Research International* 2015; 2015(1): 870389.
- Suvitha A., Periandy S., Gayathri P. NBO, HOMO–LUMO, UV, NLO, NMR and vibrational analysis of veratrole using FT-IR, FT-Raman, FT-NMR spectra and HF–DFT computational methods. *Spectrochimica Acta Part A: Molecular and Biomolecular Spectroscopy* 2015; 138: 357-369.
- Tahiroğlu V., Çimen E. 3-[1-(5-Amino-[1,3,4]tiadiazol-2-il)-2-(1H-imidazol-4-il)-etilimino]-2,3-dihidro-indol-2-on molekülün teoriksel incelenmesi. *Türk Doğa ve Fen Dergisi* 2024; 13(2): 6-13.
- Tahiroğlu V., Gören K., Bağlan M., Yıldiko Ü. Molecular docking and DFT analysis of thiazolidinone-bis schiff base for anti-cancer and anti-urease activity. *Journal of the Institute of Science and Technology* 2024; 14(2): 822-834.
- Tahiroğlu V., Gören K., Çimen E., Yıldiko Ü. Molecular docking and theoretical analysis of the (E)-5-((z)-4-methylbenzylidene)-2-(((e)-4-methylbenzylidene)hydrazineylidene)-3-phenylthiazolidin-4-one molecule. *Bitlis Eren Üniversitesi Fen Bilimleri Dergisi* 2024; 13(3): 659-672.

- Tahiroğlu V., Gören K., Yıldiko Ü., Bağlan M. Investigation, structural characterization and evaluation of the biological potency by molecular docking of amoxicillin analogue of a schiff base molecule. *International Journal of Chemistry and Technology* 2024; 8(2): 190-199.
- Taslimi P., Sujayev A., Turkan F., Garibov E., Huyut Z., Farzaliyev V., Mamedova S., Gulçin İ. Synthesis and investigation of the conversion reactions of pyrimidine-thiones with nucleophilic reagent and evaluation of their acetylcholinesterase, carbonic anhydrase inhibition, and antioxidant activities. *Journal of Biochemical and Molecular Toxicology* 2018; 32(2): e22019.
- Yildiko U., Tanriverdi AA. Synthesis and characterization of pyromellitic dianhydride based sulfonated polyimide: survey of structure properties with DFT and QTAİM. *Journal of Polymer Research* 2021; 29(1): 19.
- Yildiko U., Tanriverdi AA. A novel sulfonated aromatic polyimide synthesis and characterization: Energy calculations, QTAİM simulation study of the hydrated structure of one unit. *Bulletin of the Korean Chemical Society* 2022; 43(6): 822-835.
- Yildiko Ü., Türkan F., Tanriverdi AA., Ata AC., Atalar MN., Cakmak İ. Synthesis, enzymes inhibitory properties and characterization of 2- (bis (4-aminophenyl) methyl) butan-1-ol compound: Quantum simulations, and in-silico molecular docking studies. *Journal of the Indian Chemical Society* 2021; 98(11): 100206.
- Yu J., Jiang X. Synthesis and perspective of organosulfur chemicals in agrochemicals. *Advanced Agrochem* 2023; 2(1): 3-14.